Photonic bandgaps engineering in double graded hyperbolic, exponential and linear index materials embedded one-dimensional photonic crystals

Engineering Research Express

PAPER

Photonic bandgaps engineering in double graded hyperbolic, exponential and linear index materials embedded one-dimensional photonic crystals

RECEIVED
18 August 2019

REVISED
23 September 2019

ACCEPTED FOR PUBLICATION
27 September 2019

PUBLISHED
10 October 2019

Bipin K Singh[1], **Ashish Bijalwan**[1], **Praveen C Pandey**[2] **and Vipul Rastogi**[1]

[1] Department of Physics, Indian Institute of Technology Roorkee—247667, India
[2] Department of Physics, Indian Institute of Technology (Banaras Hindu University) Varanasi—221208, India

E-mail: bipinksingh02@gmail.com

Keywords: graded index photonic crystals, reflectance, photonic band gap

Abstract

We present the structuring of different double graded-index materials in the form of one-dimensional (1D) photonic crystals (PCs) for highly efficient light trapping and controlling photonic devices in terms of tuned and controlled photonic bandgap (PBG) performances. Considered 1D graded photonic crystal (GPC) structures are stacked of hyperbolic, exponential, and linear double graded index layers. In the graded index layers, the refractive indices vary in hyperbolic, exponential, and linear fashions as a function of the layer thickness. These configurations show that the operating frequencies and the number of PBGs can be tuned by controlling layer thickness, grading profiles, and grading parameters of the constituted graded layers. The changes in the grading profiles of the graded layers modulate the operation frequencies and also the number of PBGs. We also found that the operating frequencies and bandwidth of PBGs can be tuned by changing the values of initial and final refractive indices of the graded layer. Therefore, the desirable PBG regions and bandwidths can be achieved and controlled by selecting appropriate parameters of the systems. Results can be implemented to design tunable reflectors, multi-channel filters, sensors, and optical detectors. Also, this work may provide an understanding of the effect of different double graded-index materials on PBG characteristics in the GPCs.

1. Introduction

With a perspective to future potential applications in high-performance and light controlled photonic devices, the realization of light trapping, control, and propagation is becoming increasingly attractive. Photonic crystals (PCs) have an excellent ability to control, confine, and manipulate light with low loss. PCs are structures consisting of two or more materials of different refractive indices arranged in a periodic configuration [1, 2]. Periodic refractive index modulations prevent the propagation of electromagnetic waves in a specific frequency range known as a photonic bandgap (PBG). PBG properties are used to confine, manipulate, and manage the propagation of electromagnetic waves in the PCs, which lead to being a key technology for all integrated photonic devices [3, 4]. Several distinct structural engineering composed of different dielectric, dispersive, plasmonic, and negative index materials have been studied to control and tune the PBG characteristics efficiently [5–11]. These have several potential applications in optical communication and optoelectronic devices such as reflecting mirrors, waveguides, optical switches, filters, detectors, limiters, light-emitting diodes, etc Recently, the properties of tunable unidirectional absorption and temperature-dependent PBGs in 1D PC structures have been reported by introducing the non-magnetized/magnetized plasma and semiconductor layers [12–15]. One approach is to implement the concept of graded-index optics in PC structures to improve further the ability to control the flow of light. The different employed version of the graded-index medium in the PCs is known as a graded photonic crystal (GPC). GPCs are designed with the spatial modification of constituted parameters such as filling factor, optical index and lattice parameters, etc The spatial variations of relevant parameters in the

GPCs provide different behavior from conventional PCs and improve the ability to control and manipulate the propagation of light [16–18]. Such types of PCs play a vital role in the design of spectral filters, beam aperture and deflector, high-efficiency bending wave guides, high-efficiency couplers, self-focusing media, anti-reflection coating, etc [19–23]. In 1D PC structures, all the optical properties of electromagnetic waves are easy to investigate. These can also be designed in a controlled manner and fabricated more effectively for a broad range of wavelengths and allow for accurate theoretical descriptions. Several researchers have been proposed the 1D multilayer structures with gradual variations of refractive index and layer thickness along the perpendicular to the surface of graded layer arrangements [24–29]. Such types of structures are known as 1D GPCs. 1D GPCs are a stack of graded layers with tunable refractive index profiles which provide the additional possibility to explore the dispersion and PBGs characteristics as well as optical transmittance, reflectance, and absorbance, and group velocity, etc The physical interpretations of 1D GPCs for practical applications, a series of piecewise profile materials can obtain different types of gradation profile in the PC structures. The stratified embedded layers may be divided into a variety of sub-layers, and every sub-layer is assumed to be homogeneous. The various processes, such as chemical vapor deposition, sputtering deposition, nanolithography, and spin coating techniques, have been used to fabricate these types of structures [30–32]. It may also be possible to fabricate GPC structures by compositionally doping method [33]. The different form of graded-index media in nature, such as the graded-refractive-index structure of fish and structural colors in animals, the atmosphere of the Earth and the mirage effect, and other natural structures have been investigated. Antireflection surfaces to neutralize the boundary effect to light have also been effectively presented a gradual transition in the refractive index at the interface of two media [34].

In the present work, tunable and controlled PBG properties in double graded hyperbolic, exponential, and linear index materials embedded in 1D PC structures are expected to observe. The periodicity of double graded index layers is stacked according to the desired GPC structures. Refractive indices in graded-index layers vary in the hyperbolic, exponential and linear fashion as a function of the layer thicknesses. The following parts are included in this paper. In section II, the theory of calculating the reflectance, transmittance, dispersion spectra, reflection phase shift, group velocity, and group delay for the proposed 1D GPC structures are introduced. In section III, we present the effect of different types of dual graded-index layers and their stacking arrangements on the reflectance, dispersion spectra, reflection phase shift, group velocity, and field intensity distribution in the double graded-index slabs embedded GPC structures. The effect of the contrast of initial and final refractive index of the graded index layers on the PBG spectra is also considered. The graphical illustrations of complete photonic band gaps serve to illustrate the competitions between all of the proposed 1D GPC structures. Finally, the results are summarized and suggested their prospective applications as the photonic components in section IV.

2. Theoretical description

In order to realize the PBG engineering, we consider the double hyperbolic, exponential and linear graded index slab of thickness 2 d as constituents of the finite 1D GPC structures. GPC structures are the periodicity of a doubly hyperbolic (HH′ or H′H), exponential (EE′ or E′E), and linear (LL′ or LL′) graded index layers. Refractive indices distribution in the considered graded index layers H (E or L) and H′ (E′ or L′) vary in hyperbolically (exponentially or linearly) increasing and decreasing ways with layer thickness, respectively. The schematic of GPC structures and variations of refractive index profiles in increasing and decreasing ways with layer thickness are shown in figure 1.

In the first case, the variation of refractive index in hyperbolic graded layers is represented as [35]

$$n_H(x) = \frac{n_i}{1 - \alpha x} \tag{1}$$

where $\alpha = [(n_f - n_i)/(n_f.d)]$ is a hyperbolic grading parameter, d is the layer thickness, n_i and n_f are the initial and final refractive indices, respectively. Subscript H represents the hyperbolic graded index layer. The distribution of the electric field for electromagnetic wave propagation in a hyperbolic graded index layer along perpendicular to the surface is given as

$$E_H(x) = A_H \sqrt{\xi_H}.\cos(m.\log \xi_H) + B_H \sqrt{\xi_H}.\sin(m.\log \xi_H) \tag{2}$$

where A_H and B_H are constants for hyperbolic graded index layer, the variable $\xi_H = 1 - \alpha x$ is the propagation wave vector, and $m^2 = [(\omega n_i/c\alpha)^2 - (1/4)]$, where ω is the angular frequency, and c is the speed of light.

In the second case, the variation of refractive index in exponential graded layer is expressed as [35]

$$n_E(x) = n_i \exp(\gamma x) \tag{3}$$

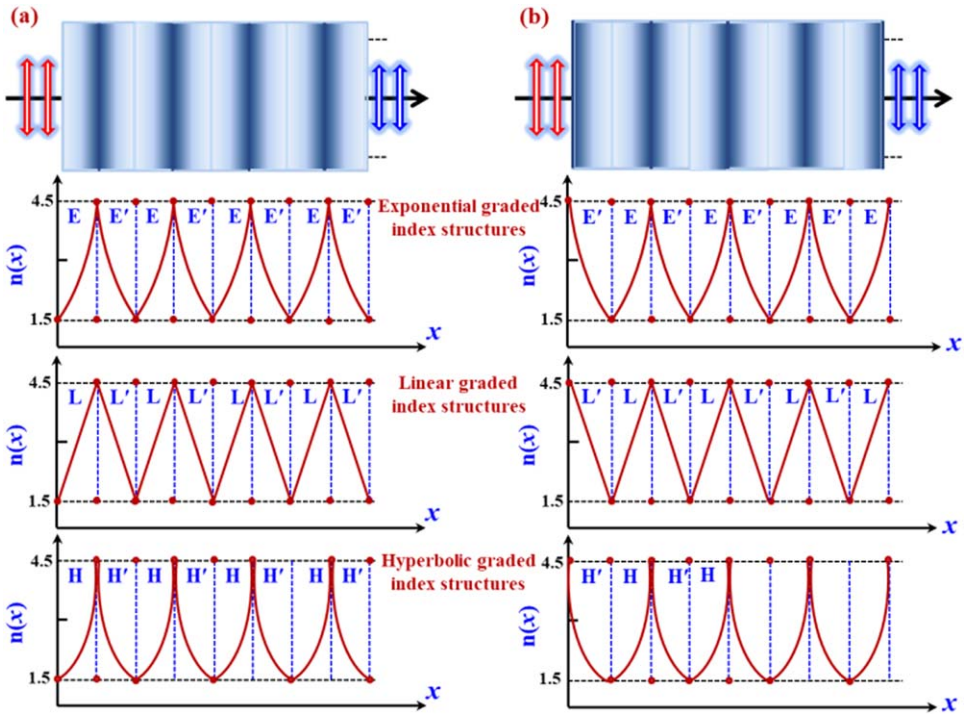

Figure 1. Schematics of the double periodic GPC structures with possible combinations of increasing and decreasing refractive index profiles in exponential, linear and hyperbolic graded index systems.

where $\gamma = (1/d).\log(n_f/n_i)$ is the exponential grading parameter, and subscript E represents the exponential graded index layer. The electric field distribution for electromagnetic wave propagation in an exponential graded index layer along the plane perpendicular to the surface of the graded layer can be written as:

$$E_E(x) = A_E.J_0\left(\frac{\xi_E}{\gamma}\right) + B_E.Y_0\left(\frac{\xi_E}{\gamma}\right) \tag{4}$$

where A_E and B_E are constants for exponential graded index layer, J_0 and Y_0 are the first and second kind of the 0^{th}-order Bessel function, respectively. The variable $\xi_E = n_E(x).\omega/c$ is the wave propagation vector for exponential graded index layer at a normal incident angle.

In the third case, the index of refraction varies linearly from initial to end boundaries of the linear graded layers and can be expressed as [35, 36]

$$n_L(x) = n_i + \left(\frac{(n_f - n_i)}{d}\right)x \tag{5}$$

The distribution of the electric field for electromagnetic wave propagation in a linear graded index layer along the plane perpendicular to the surface of the graded layer can be represented as:

$$E_L(x) = \sqrt{\xi_L}\left[A_L\, J_{1/4}\left(\frac{{\xi_L}^2}{2\beta}\right) + B_L\, Y_{1/4}\left(\frac{{\xi_L}^2}{2\beta}\right)\right] \tag{6}$$

where A_L and B_L are the constants for the linear graded index layer, the functions $J_{1/4}$ and $Y_{1/4}$ are first and second kind of the $(1/4)^{th}$-order Bessel function, respectively. The variable $\beta = (\omega/c).[(n_f - n_i)/d]$ is a linear grading parameter, and $\xi_L = n_L(x).\omega/c$ is the wave propagation vector for the linear graded layers at a normal incident angle. The variations of the refractive index can be changed according to increasing or decreasing fashion by considering the values of initial (n_i) to end (n_f) boundaries refractive index of the graded index layers as illustrated in figures 1(a) and (b), respectively. For increasing index profile in the graded layers (H, E, and L), the values of refractive index increase with layer thickness from refractive index $n_i = 1.5$ to $n_f = 4.5$. For decreasing index profile in the graded layers (H′, E′, and L′), the values of refractive index decrease with layer thickness from refractive index $n_i = 4.5$ to $n_f = 1.5$. The expressions for the distribution of electric field in the corresponding graded index layers would be in the same form for increasing or decreasing index profile except for the grading parameters which will change according to the variation of refractive index in the graded layers.

We have embraced multilayer interface optics to calculate optical properties such as reflection, transmission, phase shift, dispersion relationship, group velocity, time delay and field distributions for the proposed GPC structures. In order to achieve the complete reflectance (R) and transmittance (T) spectra, it is essential to

calculate the reflection (r), and transmission (t) coefficients of the fields in the incident and outgoing media attributable to partially transmitted and reflected waves originated within the multilayer structures at each layer interface. The frequency dependent field coefficients A_l and B_l ($l = 0, 1, 2, 3 \ldots$) are expressed transmitted and reflected waves amplitudes, respectively. These field coefficients are calculated by imposing continuity conditions for both the electric and the magnetic field across the interface from one medium to the next medium. Then, a set of equations is established from the transfer matrix approach. To investigate the optical properties of the light wave propagation in the doubly periodic graded index multilayer structures, we have used the transfer matrix formulism. After applying the transfer matrix approach in the proposed structures, the light wave propagation through the complete structures can be expressed by multiplying the characteristic matrices of the embedded graded layers in the doubly periodic GPC structures. The complete characteristic matrix expression for the doubly periodic GPC structures can be expressed as

$$\begin{pmatrix} A_0 \\ B_0 \end{pmatrix} = M_0^{-1}.[(M_G.M'_G) \; or \; (M'_G.M_G)]^N.M_0 \begin{pmatrix} A_{N+1} \\ 0 \end{pmatrix} \tag{7}$$

where N is the number of periods, and A_0, B_0, and A_{N+1} are the constant for the incident (0^{th}) and outgoing ($N+1$)th media, respectively. The matrices M_G and M'_G are the 2×2 characteristic matrices for increasing and decreasing refractive index profiles in the different graded index layers, respectively. Subscript G represents for graded index layers. The matrix M_0 is 2×2 characteristic matrix of air medium. The characteristic matrix is $M_G = M_i.M_f^{-1}$, where matrices M_i and M_f are the characteristic matrices at the initial ($n_i = 1.5$) and the end ($n_f = 4.5$) boundaries of the graded index layers with increasing the refractive index profiles. Similarly, the characteristic matrix is $M'_G = M'_i.M'^{-1}_f$, where matrices M'_i and M'_f are the characteristic matrices at the initial ($n_i = 4.5$) and the end ($n_f = 1.5$) boundaries of the graded index layers with decreasing the refractive index profiles. The characteristics matrices at the initial (M_i and M'_i) and final (M_f and M'_f) boundaries of the graded layers can be changed according to the hyperbolic, exponential and linear graded-index media. After simplify the sets of field expressions and established the matrix expressions, the characteristic matrices M_i and M_f at the initial and final boundaries of the hyperbolic graded-index media in the GPC structures at a normal incident angle are obtained as

$$M_i = \begin{pmatrix} 1 & 0 \\ \alpha/2 & \alpha.m \end{pmatrix} \text{and } M_f = \begin{pmatrix} \sqrt{\frac{n_i}{n_f}}.\cos(z_H) & \sqrt{\frac{n_i}{n_f}}.\sin(z_H) \\ -\frac{\alpha}{2.\sqrt{\frac{n_i}{n_f}}}[2m.\sin(z_H) - \cos(z_H)] & \frac{\alpha}{2.\sqrt{\frac{n_i}{n_f}}}[2m.\sin(z_H) + \cos(z_H)] \end{pmatrix}$$

where $z_H = m.\log\left(\frac{n_i}{n_f}\right)$, n_i and n_f are the refractive indices at the initial and final edges of the exponential graded layer, respectively. The characteristic matrices M_i and M_f at the initial and final boundaries of the exponential graded index layers are expressed as

$$M_i = \begin{pmatrix} J_0\left(\frac{\xi_i}{\gamma}\right) & Y_0\left(\frac{\xi_i}{\gamma}\right) \\ \xi_i J_1\left(\frac{\xi_i}{\gamma}\right) & \xi_i Y_1\left(\frac{\xi_i}{\gamma}\right) \end{pmatrix}$$

and

$$M_f = \begin{pmatrix} J_0\left(\frac{\xi_f}{\gamma}\right) & Y_0\left(\frac{\xi_f}{\gamma}\right) \\ \xi_f J_1\left(\frac{\xi_f}{\gamma}\right) & \xi_f Y_1\left(\frac{\xi_f}{\gamma}\right) \end{pmatrix}$$

where the wave vectors are $\xi_i = \omega n_i / c$ at the initial and $\xi_f = \omega n_f / c$ at the final boundaries. The functions $J_{0(1)}$ and $Y_{0(1)}$ are first and second kind of the 0th-order (1st-order) Bessel functions, respectively. The characteristic matrices M_i and M_f at the initial and final boundaries of the linear graded-index media are obtained as [28]

$$M_i = \begin{pmatrix} \sqrt{\xi_0}.J_{\frac{1}{4}}\left(\frac{\xi_0^2}{2\beta}\right) & \sqrt{\xi_0}.Y_{\frac{1}{4}}\left(\frac{\xi_0^2}{2\beta}\right) \\ -\left(\frac{\beta}{2{\xi_0}^{3/2}}.J_{\frac{1}{4}}\left(\frac{\xi_0^2}{2\beta}\right) + {\xi_0}^{3/2}.J'_{\frac{1}{4}}\left(\frac{\xi_0^2}{2\beta}\right)\right) & -\left(\frac{\beta}{2{\xi_0}^{3/2}}.Y_{\frac{1}{4}}\left(\frac{\xi_0^2}{2\beta}\right) + {\xi_0}^{3/2}.Y'_{\frac{1}{4}}\left(\frac{\xi_0^2}{2\beta}\right)\right) \end{pmatrix}$$

and

$$M_f = \begin{pmatrix} \sqrt{\xi_1}.J_{\frac{1}{4}}\left(\frac{\xi_1^2}{2\beta}\right) & \sqrt{\xi_1}.Y_{\frac{1}{4}}\left(\frac{\xi_1^2}{2\beta}\right) \\ -\left(\frac{\beta}{2{\xi_1}^{3/2}}.J_{\frac{1}{4}}\left(\frac{\xi_1^2}{2\beta}\right) + {\xi_1}^{3/2}.J'_{\frac{1}{4}}\left(\frac{\xi_1^2}{2\beta}\right)\right) & -\left(\frac{\beta}{2{\xi_1}^{3/2}}.Y_{\frac{1}{4}}\left(\frac{\xi_1^2}{2\beta}\right) + {\xi_1}^{3/2}.Y'_{\frac{1}{4}}\left(\frac{\xi_1^2}{2\beta}\right)\right) \end{pmatrix}$$

where the functions $\xi_i = \omega n_i/c$ and $\xi_f = \omega n_f/c$ are the wave vectors at the initial and final edges of the linear graded index layers, respectively. The functions $J_{1/4}$ and $Y_{1/4}$ are the first and second kind of the 1/4th-order Bessel functions, and the functions $J'_{1/4}$ and $Y'_{1/4}$ are the differential of the first and second kind of the 1/4th-order Bessel functions, respectively. The characteristic matrix of air medium is given as

$$M_0 = \begin{pmatrix} 1 & 1 \\ ik_0 & -ik_0 \end{pmatrix}$$

where k_0 $(= n_0.\omega/c)$ is the wave vector of air medium, and n_0 is the refractive index of the air. For the reverse case of the variations of refractive index in the graded index layers, the characteristic matrices (M'_i and M'_f) at the initial and final boundaries would be in the same form for the respective graded-index media except for the values of refractive indices $n_i = 4.5$ and $n_f = 1.5$. The magnitude of the forwarding and backward collected light waves of the GPC structure can be calculated from a simple matrix operation as given in the equation (7). In this way, the reflection (r) and transmission (t) coefficients of the structures can be obtained directly. The phase shift of the electromagnetic wave in the PC based optical devises is also one of particular interest. The reflectance (R), transmittance (T) and reflection phase shift (Ψ) of the periodic structures can be calculated using the following relations [35, 36]

$$\left.\begin{array}{c} \mathrm{R} = |\mathrm{r}|^2 = \left|\frac{\mathrm{B}_0}{\mathrm{A}_0}\right|^2 \text{ and } \mathrm{T} = |\mathrm{t}|^2 = \left|\frac{\mathrm{A}_{\mathrm{N}+1}}{\mathrm{A}_0}\right|^2 \\ r = |r|.\exp(-i\Psi) \end{array}\right\} \tag{8}$$

A periodic multilayer structure is equivalent to a 1D periodic lattice arrangement, which is invariant under the lattice translation. Here, the refractive indices of graded layers are invariant by the revealing of the wave vector by a lattice constant $2d$ for the doubly periodic GPC structures. According to the Floquet's theorem, the electric field vector in a periodic system takes the form as: $E_K(x + 2d) = E_K(x)$ with period 2 d. The dispersion relation is an equation relating the Bloch wave number K and angular frequency ω for a periodic system, which is derived for an infinite periodic structure using the transfer matrix approach as

$$K(\omega) = \frac{1}{2d}.\cos^{-1}\left\{\frac{1}{2}(M_{11} + M_{22})\right\} \tag{9}$$

where $2d$ is the thickness of a period of the periodic system, M_{11} and M_{22} are the elements of the 2×2 optical transfer matrix $M_{i,j}(i, j = 1, 2)$ of a period. The optical transfer matrix may be $M_{i,j} = M_G M'_G$ or $M'_G M_G$ according to the considered doubly periodic GPC structures. The dispersion spectra reveal multiple spectral bands categorized into two regimes. First, the place $|(M_{11} + M_{22})/2| \leqslant 1$ corresponds to real K value implies to propagating electromagnetic waves. Second, spectral band regions within which K is complex correspond to the evanescent waves which are attenuated the wave propagation and defined by the condition $|(M_{11} + M_{22})/2| > 1$. These bands correspond to the forbidden bands of the systems known as photonic band-gaps. The group velocity and group time delay of electromagnetic waves in various periodic structures with different types of materials have also been attracted the researcher's attention on control and manipulation of light in photonic structures. Equation (9) leads directly to calculate the group velocity (v_g) and group delay (τ) which have the expression as [35, 36]

$$v_g = \frac{d\omega}{dK} = \left[\frac{dK}{d\omega}\right]^{-1} \text{ and } \tau = \frac{2d}{v_g} \tag{10}$$

The group velocity and time delay of the radiation modes have a significant role in light propagation and optical response in the optical structures.

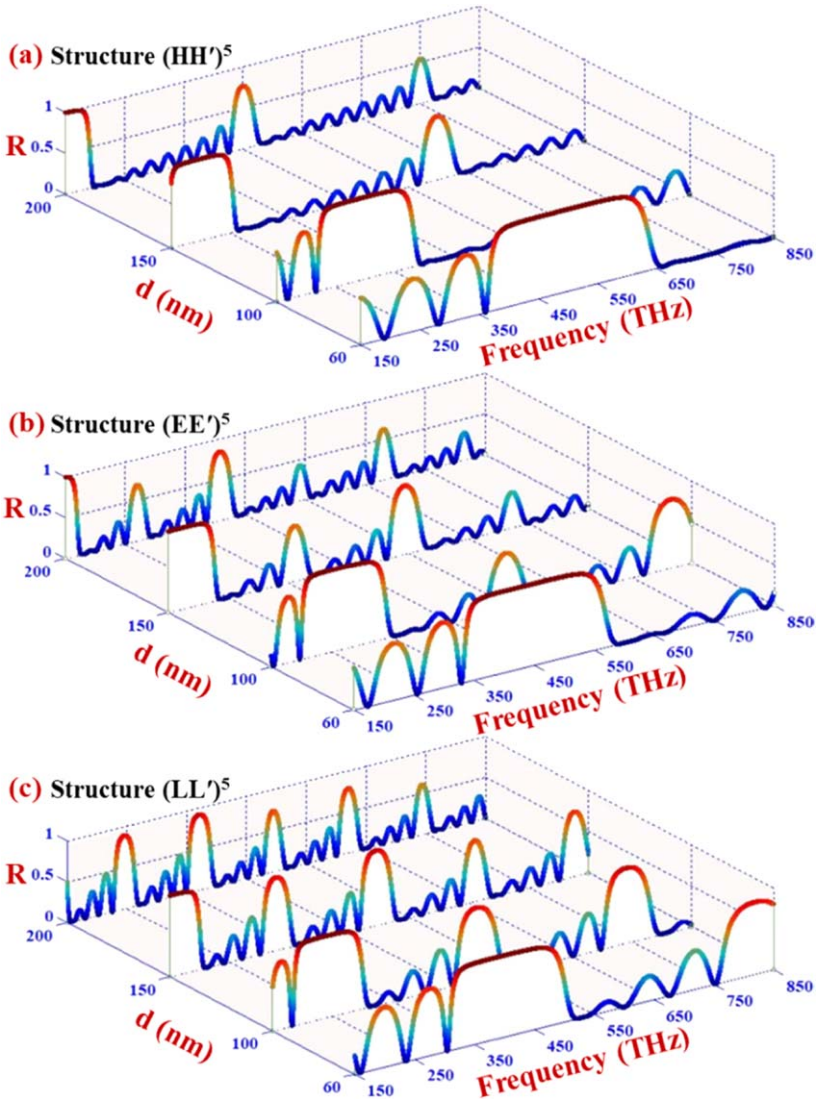

Figure 2. Reflectance spectra for double GPC structures with the periodicity of (a) hyperbolic HH′, (b) exponential EE′ and (c) linear LL′ graded index systems for different layer thicknesses.

3. Numerical results and discussion

Here we present the numerical results for the doubly periodic GPC structures to characterize the optical reflection, band structures, phase shift, group speed, and time delay. The graded-index media is presumed to be lossless dielectrics. Refractive indices of the graded-index media are considered between lower refractive index 1.5 to upper refractive index 4.5. The refractive index variations with the layer thickness in a unit cell are the combinations of increasing and decreasing index layers, as shown in figure 1. The GPC structures are fabricated with the periodicity of HH′ (or H′H) for hyperbolic, EE′ (or E′E) for exponential and LL′ (or L′L) for linear graded index layers. The reflection spectra for the periodicity of five sets of hyperbolic graded systems (HH′ and H′H), exponential graded systems (EE′ and EE′), and linear graded systems (LL′ and L′L) are shown in figures 2 and 3 for different layer thicknesses, respectively. It is observable from the results shown in the figures that there exist a number of forbidden (photonic) bands. The number of PBGs increases with layer thickness and reduces the corresponding bandwidth. These PBG properties are mainly affected by the effective refractive index of the constituted media in the PC structures. The effective refractive index of the graded layer becomes more significant as the layer thickness increases, and hence the Bragg structure becomes more effective to create PBGs. We also notice that the PBGs of GPC structures significantly depend on the grading profiles.

In the case of figure 2, reflection band amplitudes and bandwidths change with increasing the number of PBGs with layer thickness. It is the consequence of decreasing the average effective refractive indices over the volume of embedded graded-index systems. In the second case of figure 3, reflection band amplitudes are comparatively higher from the first case. It is perceptible that the corresponding reflection band regions are

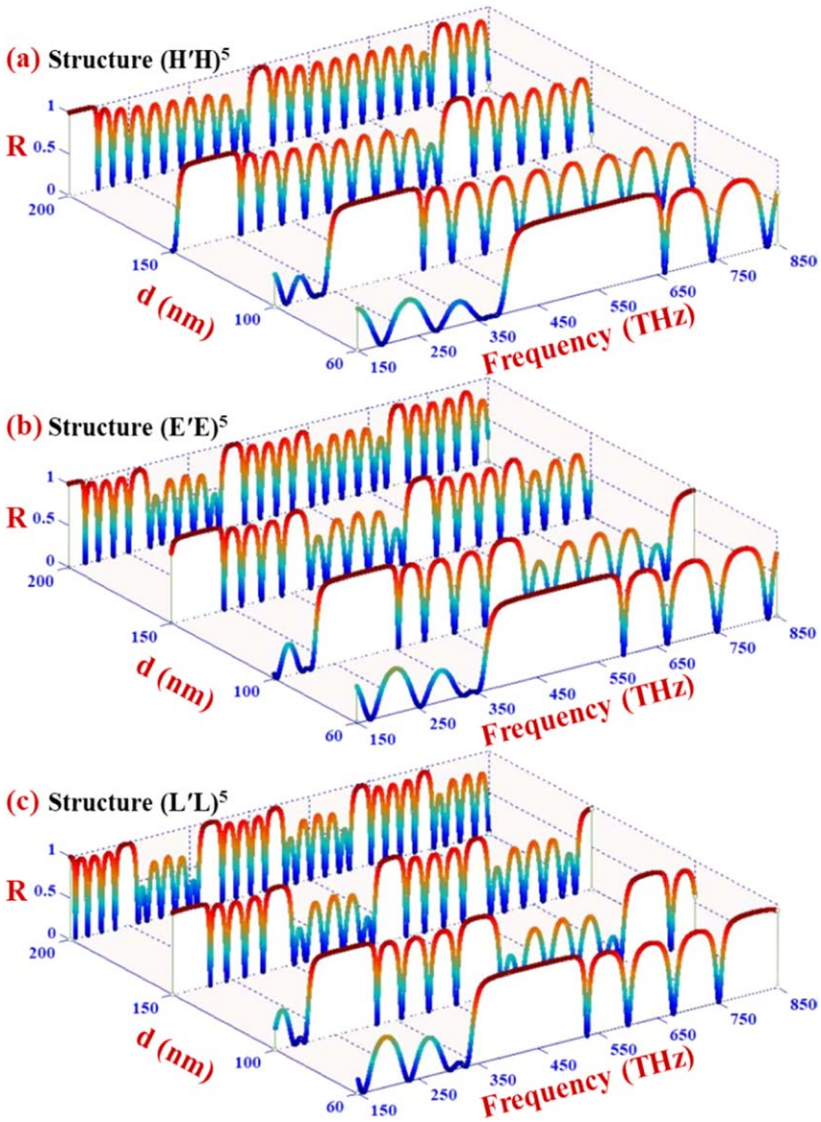

Figure 3. Reflectance spectra for double GPC structures with the periodicity of (a) hyperbolic H′H, (b) exponential E′E and (c) linear L′L graded index systems for different layer thicknesses.

almost the same for both the cases. The reflection bands shift downward in frequency regions and their bandwidths usually shorter for the structures with hyperbolic, exponential, and linear graded-index systems, respectively. For layer thickness d = 60 nm, the band region and bandgap for hyperbolic GPC structures are obtained to be 399.3–623.8 THz and 224.5 THz, respectively. The band region shifts toward lower frequencies and the corresponding bandwidth reduce when the refractive index profile changes from hyperbolic to exponential (or linear). The changes in the reflection spectra for the combinations of increasing and decreasing graded index profiles are the consequences of different saw-tooth index profiles formations. One way is to tailor to different types of gradation profile in the PC structures can be obtained by a series of piecewise hyperbolic, exponential and linear index profile materials. It can also be seen that the reflection spectra of the 1st case of GPC structures exhibit high amplitude reflection band as compared to the other ripples amplitude which is significant and useful for optical filtering applications. In the 2nd case of GPC structures, the spectra exhibit many ripples with high amplitudes. The ripples have to be reduced considerably to suit filter applications.

For the higher layer thickness, we notice that some of the reflection bands cannot easily designate. We have therefore analyzed the confinement effects arising from the competition between changing of layer thickness and PBG band region in the dispersion spectra. The calculated frequency regions of PBGs at different layer thickness are shown in figure 4 for the GPC structures with hyperbolic, exponential, and linear graded-index systems. The figure shows the distribution of the PBGs (black regions) and allowed (white region) frequency regions as a function of the graded layer thickness. As the graded layer thickness increases, we get the number of PBGs, and their bandwidths become narrower and narrower with increasing the number of PBGs. We observe that the generation of PBGs is almost the same for both types of double periodic GPC structures. The

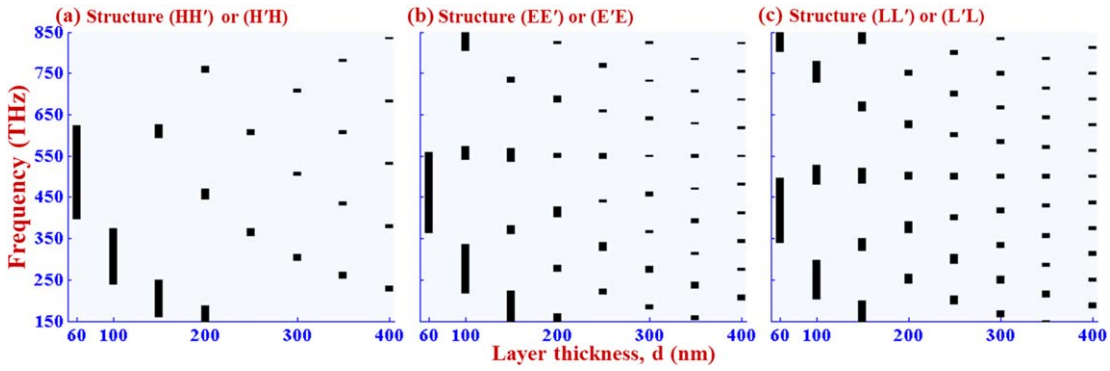

Figure 4. Distributions of photonic band gap (black region) as a function of layer thickness *d* for the periodicity of (a) hyperbolic HH′ or H′H, (b) exponential EE′ or E′E, and (c) linear LL′ or L′L graded index systems.

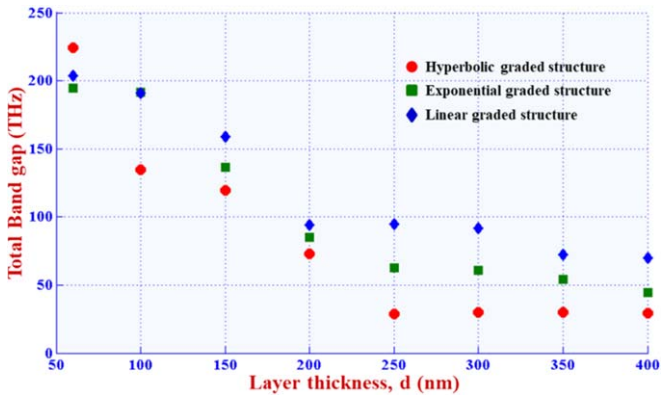

Figure 5. Variations of total band gap regions against the layer thickness *d* for the doubly periodic hyperbolic, exponential and linear GPC structures.

bandwidths and band regions of PBGs have different values for the different graded-index media. We observe the more significant number of PBGs and their bandwidths become very shorter. The variations in the PBGs are the consequence of the changes of average volume-effective refractive index for different graded-index systems, while lower and higher values of refractive index are the same. The combinations of increasing and decreasing gradation profiles for different graded-index media show the significant influences on bandwidth and band region of PBGs. We observe that the dispersion spectra and formations of PBGs are similar for both types of combinations of increasing and decreasing gradation profiles graded-index media.

The variations of total bandwidths with layer thickness for the structures with different graded-index systems are depicted in figure 5. It reveals that the values of total bandgaps have significant change with the layer thicknesses. The values of the total band gap usually reduce for the structures with linear, exponential, and hyperbolic graded-index systems, respectively. Therefore, PBGs can be tuned with layer thickness and grading profiles in the GPC structures. Table 1 lists the PBGs region and their bandwidth for the proposed doubly periodic GPCs at different layer thickness.

We extend our study to calculate the dispersion spectra and reflection phase shift (Ψ) associated with PBGs in the doubly periodic GPC structures with different graded-index systems. The calculated dispersion spectra and corresponding reflection phase shifts are illustrated in panels (i), (ii) and (iii) of figure 6 for the structures with the periodicity of hyperbolic graded system HH′ or H′H, exponential graded system EE′ or E′E, and linear graded system LL′ or L′L, respectively. We observed that the results of the dispersion spectra are similar for both types of combinations, whereas reflection phase shifts change with the combination of different gradation profiles. As expected, PBGs are formed in zero transmission range and shift toward lower frequency region for the structures with hyperbolic, exponential, and linear graded-index systems, respectively. The photonic band regions are depicted by gray region in dispersion spectra. It can be seen that three PBGs are formed in the case of GPC structures with exponential and linear graded-index systems, whereas two PBGs are visible for the GPC structures with hyperbolic graded-index systems. The bandwidth of second-order PBG in the hyperbolic graded-index systems is approximately negligible. The reflection phase shifts are illustrated in panels (ii) and (iii)

Table 1. Band region and bandwidth of PBGs for the doubly periodic GPC structures with different graded index systems.

Layer Thickness, d		Periodic structure of graded system					
		HH′ or H′H		EE′ or E′E		LL′ or L′L	
		Band region (THz)	Band gap (THz)	Band region (THz)	Band gap (THz)	Band region (THz)	Band gap (THz)
60 nm	1st	399.3–623.8	224.5	364.6–559.3	194.7	339.6–497.3	157.7
	2nd	—	—	—	—	804.2–850.0	45.8
100 nm	1st	239.6–374.3	134.7	805.7–850.0	44.3	728.0–779.9	51.9
	2nd	—	—	541.5–572.0	30.5	482.5–527.0	44.5
	3rd	—	—	218.8–335.6	116.8	203.7–298.4	94.7
150 nm	1st	595.8–625.4	29.6	729.5–741.1	11.6	823.3–847.7	24.4
	2nd	159.8–249.5	89.7	537.1–568.2	31.1	658.6–679.8	21.2
	3rd	—	—	361.0–381.3	20.3	485.3–519.9	34.6
	4th	—	—	150.0–223.7	73.7	321.7–351.3	29.6
	5th	—	—	—	—	150.0–198.9	48.9
200 nm	1st	753.6–767.0	13.4	822.5–828.4	5.9	745.4–757.6	12.2
	2nd	446.8–469.1	22.3	681.1–695.6	14.5	617.5–635.7	18.2
	3rd	150.0–187.1	37.1	547.1–555.8	8.7	493.9–509.8	15.9
	4th	—	—	402.9–426.1	23.2	364.0–389.9	25.9
	5th	—	—	270.8–286.0	15.2	241.3–263.5	22.2
	6th	—	—	150.0–167.8	17.8	—	—

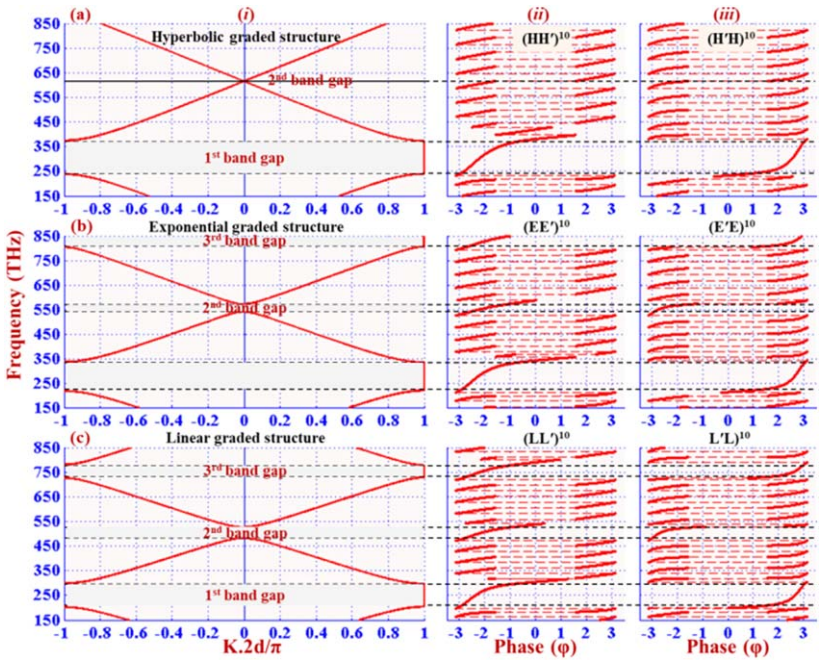

Figure 6. Panel (i) shows the dispersion spectra for both types of the double periodic arrangements for (a) hyperbolic, (b) exponential and (c) linear graded index systems, and panels (ii) and (iii) illustrate the reflection shift for the structures with possible combinations of increasing and decreasing gradation profiles graded systems.

for the periodic structures of systems HH′, EE′, LL′ and H′H, E′E, L′L systems, respectively. The changes in the reflective phase shift from $-\pi$ to $+\pi$. The variations of reflection phase shifts are different for various PBGs. The reflection phase shifts for the periodic hyperbolic (HH′), exponential (EE′) and linear (LL′) graded-index systems change smoothly from close to $-\pi$ at one band edge to approximate 0 at another band edge of PBG as shown in panel (ii). For the periodic hyperbolic (H′H), exponential (E′E) and linear (L′L) graded-index systems, the values of reflection phase shifts change from close to 0 to $+\pi$ at the edges of PBGs as depicted in panel (iii). It is the result of field distribution variability owing to different combinations of gradation profiles. The field distributions change according to the hyperbolic, exponential, and linear gradation profiles. Therefore, the

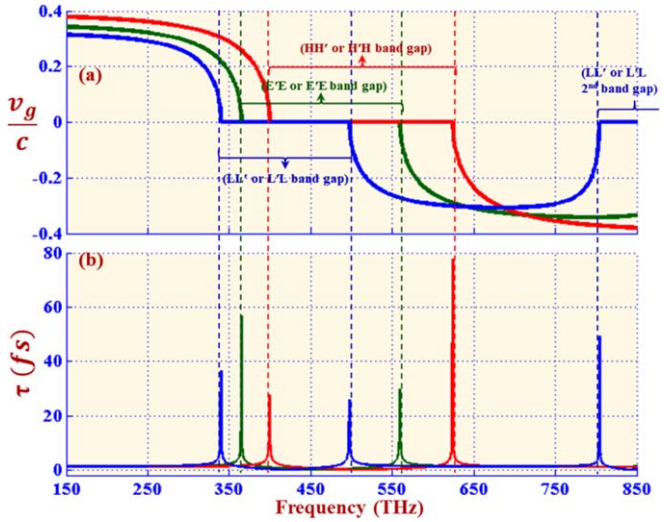

Figure 7. Panels (a) and (b) show the variation of group velocities (v_g) in unit c (light velocity) and group time delay (τ) for the considered double periodic GPC structures with layer thickness $d = 60$ nm.

transformations of field distribution in the different gradation profiles systems at the interface boundaries lead to the change of reflection phase shifts in PBG regions.

To investigate the effect of the combination of different grading profiles on the propagation light in the proposed structures, we have also calculated the group velocity and group delay for layer thickness. The measured group velocity and time delay for the GPC strictures with hyperbolic, exponential, and linear graded-index systems are shown in figure 7. Three different color lines represent the calculated results of group velocity and delay time derived for the structures with hyperbolic, exponential, and linear graded-index systems. By examining the group velocities, as shown in figure 7(a), it is apparent that the group velocities demonstrate positive and negative values outside of the PBG regions and forbidden in PBG regions. As expected, the PBG regions shift serially toward higher frequency region for the structures with linear, exponential, and hyperbolic graded-index systems. The maximum and minimum values of positive and negative group velocities also increase and shift toward lower frequency for the structures with hyperbolic, exponential, and linear graded-index systems, respectively. The effects of the combination of different grading profiles on the properties of light propagation are also described by measuring the delay time for the proposed structures. Figure 7(b) shows the calculated group delay times for the structures with different graded-index systems at layer thickness $d = 100$ nm. We note that the group delay time (τ) with femtosecond (fs) unit is minimal at the center of PBGs. Group delay time stretches sharply with high values at the edges of PBG where group velocity changes rapidly with frequency. The aspect of minimum values of time delay is a consequence of the minimum optical penetration into the structures at the center of PBGs. Group delay times under the PBG regions are also shifted downward to the frequency and have different peak values at the edges of PBGs for the strictures with hyperbolic, exponential and linear graded-index systems, respectively. The distinct peak values of group time delay at the lower and higher band edges of PBGs for the various proposed structures are a result of the change of the group velocities under the influence of the different gradation profiles. Thus, the group velocity and delay time can also be modulated as the combination of the different grading index profiles. Moreover, we observed that the group velocities and group delay times are invariant for the arrangement of increasing and decreasing gradation profiles in the GPC structures.

In order to better realization of the effects of the combination of different grading profiles on the propagation of light in the double periodic GPC structures, we have calculated the spatial distribution of the squared magnitude of the electric field $E(x)$ at selected frequencies that impinge at the 100% and 0% reflection conditions for the GPC structures. The results are shown in figure 8. Panels (i) and (ii) of the figure respectively show the variation of field intensities for the structures with a periodicity of the two possible combinations of increasing and decreasing gradation profiles of the proposed graded-index media. The effects of the combination of gradation profiles on the distribution of the electric field for $d = 200$ nm are significantly noticeable. We have selected the frequencies 600 THz and 663.4 THz for hyperbolic, 800 THz and 769.8 THz for exponential and 750 THz and 700.9 THz for linear graded-index systems stacked GPCs where maximum ($\approx$100%) and minimum ($\approx$0%) reflection conditions are satisfied. The electric field intensity distributions within the proposed structures at the selected frequencies are demonstrated in figure 8. It is found that the electric field intensities change due to changing the values of reflection and transmission coefficients under the

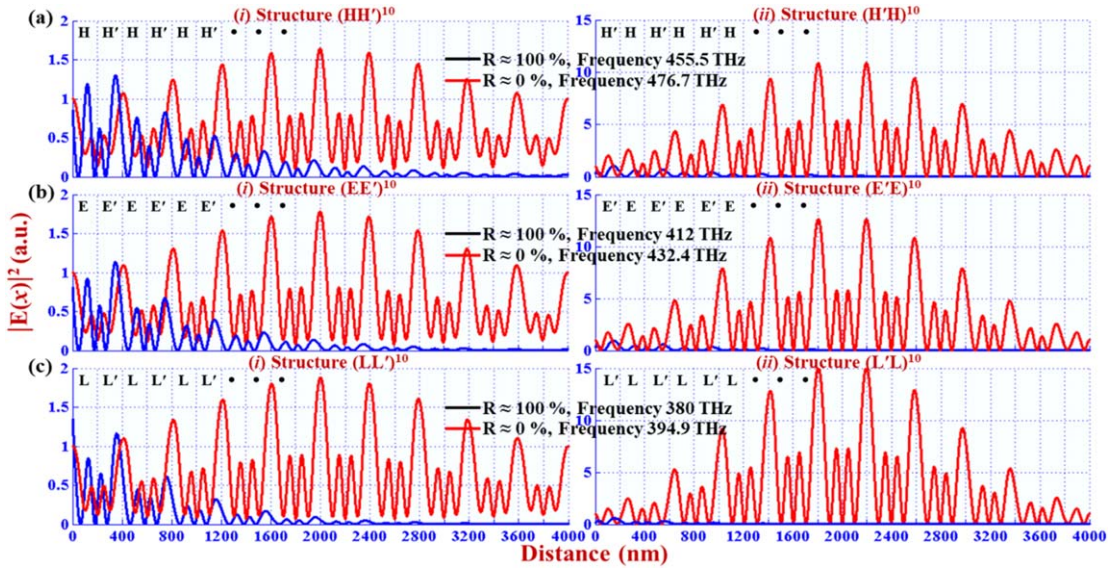

Figure 8. The distributions of electric field intensity in the doubly periodic systems of (a) hyperbolic, (b) exponential and (c) linear graded index media with two possible combinations of increasing and decreasing gradation profiles graded layers with thickness $d = 200$ nm.

influence of the different combinations of grading profiles. For different combinations of grading profiles, the filed distributions are also having different form and intensities values, although the initial and final refractive indices of the graded media are the same. The field intensities for the arrangements with the periodicity of HH′, EE′, and LL′ systems show the higher values as compared to the arrangements with the periodicity of H′H, E′E, and L′L systems, as clearly visible in the figure. The field intensities concentrate maximum energy within the structures for 0% reflection condition while its change with propagation depth by increasing the value of reflection coefficients, and its approach to negligible for 100% reflection condition for all the cases.

4. Conclusion

In this work, We have investigated the influence of different graded-index media on the optical reflectance, dispersion spectra, phase shift, group velocity, delay time and field distribution which conclude the photonic characteristics in the 1D double periodic GPC structures. It is found that the operating frequencies and the generation of a number of PBGs can be modulated considering into account the different grading profiles and their arrangements. The number of multi-channel PBGs increases with layer thickness. The band region and bandwidth of PBGs can be tuned by controlling lattice parameters, grading parameters, and profiles. The bandwidths of PBGs are strongly dependent on grading profiles. The variations in band region and bandwidth of PBGs are distinct for different grading index profiles and their arrangements as the saw-tooth index profiles. The changes in the operating frequencies of PBGs are generally shifted toward lower frequency respectively for the structures with hyperbolic, exponential, and linear graded-index media. We have also demonstrated the substantial influence on the reflection phase shift, electric field distribution, group velocity, and delay time for the proposed GPC structures. As the interference magnitude changes with the number of unit cells and different grading profiles, we observe the noticeable changes in group velocity and delay time with crystal length. The unique change in the photonic properties points to the possibility of various photonic applications. We can tune and achieve the desired photonic characteristics by selecting the necessary parameters in the proposed GPCs. GPCs can be utilized to design various photonic devices such as mirrors, multi-channel filters, optical sensors, and other photonic devices. This research will also reveal a layout of understanding the effect of different saw-tooth grading profiles on the photonic properties in the different GPC structures.

Acknowledgments

One of the authors (B K Singh) is thankful for providing financial support in the form of a national postdoctoral fellowship to the Department of Science and Technology, India.

ORCID iDs

Bipin K Singh https://orcid.org/0000-0002-7780-8521

References

[1] Yablonovitch E 1987 Inhibited spontaneous emission in solid-state physics and electronics *Phys. Rev. Lett.* **58** 2059–62
[2] Joannopoulos J D, Villeneuve P R and Fan S 1997 Photonic crystals: putting a new twist on light *Nature* **386** 143–59
[3] Lipson R H and Lu C 2009 Photonic crystals: a unique partnership between light and matter *Eur. J. Phys.* **30** S33–48
[4] Joannopoulos J D, Johnson S G, Winn J N and Meade R D 2008 *Photonic Crystals: Molding flow of light* (Princeton, New Jersey: Princeton University Press)
[5] Tolmachev V A, Perova T S, Ruttle J and Khokhlova E V 2008 Design of one-dimensional photonic crystals using combination of band diagram and photonic gap map approaches *J. Appl. Phys.* **104** 033536
[6] Negro L D, Yi J H, Nguyen V, Yi Y, Michel J and Kimerling L C 2005 Spectrally enhanced light emission from aperiodic photonic structures *Appl. Phys. Lett.* **86** 261905
[7] Zhou L, Song Z, Huang X and Chan C T 2012 Physics of the zero-n photonic gap: fundamentals and latest developments *Nanophotonics* **1** 181–98
[8] Vasconcelos M S, Mauriz P W, de Medeiros F F and Albuquerque E L 2007 Photonic band gaps in quasiperiodic photonic crystals with negative refractive index *Phys. Rev.* B **76** 165117
[9] Singh B K and Pandey P C 2014 A study of optical reflectance and localization modes of 1D Fibonacci photonic quasicrystals using different graded dielectric materials *J. Mod. Opt.* **61** 887–97
[10] Yu Z, Wang Z and Fan S 2007 One-way total reflection with one-dimensional magneto-optical photonic crystals *Appl. Phys. Lett.* **90** 121133
[11] Singh B K and Pandey P C 2014 Influence of graded index materials on the photonic localization in one-dimensional quasiperiodic (Thue–Mosre and Double-Periodic) photonic crystals *Opt. Commun.* **333** 84–91
[12] Ma Y, Zhang H, Zhang H, Liu T and Li W 2018 Properties of unidirectional absorption in one-dimensional plasma photonic crystals with ultra-wideband *Appl. Opt.* **57** 8119–24
[13] Ma Y, Zhang H, Liu T and Li W 2019 Study on the properties of unidirectional absorption and polarization splitting in one dimensional plasma photonic crystals with ultra-wideband *J. Opt. Soc. Am.* B **35** 2250–9
[14] Zhang H F, Ma Y, Li W Y and Liu T 2019 Investigation of unidirectional ultra-wideband absorption in the one-dimensional plasma photonic crystals with Thue-Morse sequence *Phys. Plasmas* **26** 012112 (14 pp)
[15] Singh B K and Pandey P C 2016 Effect of temperature on terahertz photonic and omnidirectional band gaps in one-dimensional quasi-periodic photonic crystals composed of semiconductor InSb *Appl. Opt.* **55** 5684–92
[16] Centeno E and Cassagne D 2005 Graded photonic crystals,' *Opt. Lett.* **30** 2278–80
[17] Kurt H and Citrin D S 2007 Graded index photonic crystals *Opt. Express* **15** 1240–53
[18] Lin S C S, Huang T J, Sun J H and Wu T T 2009 Gradient index photonic crystals *Phys. Rev.* B **79** 094302
[19] Lu M, Juluri B K, Lin S C S, Kiraly B, Gao T and Huang T J 2010 Beam aperture modifier and beam deflector using gradient-index photonic crystals *J. Appl. Phys.* **108** 103505
[20] Wang H W and Chen L W 2011 High transmission efficiency of arbitrary waveguide bends formed by graded index photonic crystals,' *JOSA* B **28** 2098–104
[21] Cakmak A O, Colak E, Caglayan H, Kurt H and Ozbay E 2009 High efficiency of graded index photonic crystal as an input coupler *J. Appl. Phys.* **105** 103708
[22] Vasic B and Gajic R 2011 Self-focusing media using graded photonic crystals, fourier transforming and imaging, directive emission, and directional cloaking *J. Appl. Phys.* **110** 053103
[23] Wang H W and Chen L W 2011 A cylindrical optical black hole using graded index photonic crystals *J. Appl. Phys.* **109** 103104
[24] Rauh H, Yampolskaya G I and Yampolskii S V 2010 Optical transmittance of photonic structures with linearly graded dielectric constituents *New J. Phys.* **12** 073033
[25] Sang Z F and Li Z Y 2006 Optical properties of one-dimensional photonic crystals containing graded materials *Opt. Commun.* **259** 174–8
[26] Rauh H, Yampolskaya G I and Yampolskii S V 2012 Optical transmittance of photonic structures with logarithmically similar dielectric constituents *J. Opt.* **14** 015101
[27] Ribeiro P and Raposo M 2016 Photoptics 2015 119–44(Switzerland: Springer International Publishing)
[28] Singh B K, Chaudhari M K and Pandey P C 2016 Photonic and omnidirectional band gap engineering in one-dimensional photonic crystals consisting of linearly graded index material *J. Lightwave Technol.* **34** 2431–8
[29] Singh B K and Pandey P C 2018 Tunable temperature-dependent THz photonic band gaps and localization mode engineering in 1D periodic and quasi-periodic structures with graded-index materials and InSb *Appl. Opt.* **57** 8171–81
[30] Park J H, Choi W S, Koo H Y and Kim D Y 2005 Colloidal photonic crystal with gradedrefractive-index distribution *Adv. Mater.* **17** 879–85
[31] Aytug T *et al* Monolithic graded-refractive-index glass-based antireflective coatings: broadband/omnidirectional light harvesting and self cleaning characteristics *Journal of Materials Chemestry* C **3** 2015 5440–9
[32] Gaufillet F and Akmansoy E 2013 Design and experimental evidence of a flat graded-index photonic crystal lens *J. Appl. Phys.* **114** 083105-1–083105-5
[33] Chhajed S, Schubert M F, Kim J K and Schubert E F 2008 Nanostructured multilayer graded-index antireflection coating for Si solar cells with broadband and omnidirectional characteristics *Appl. Phys. Lett.* **93** 251108 (3 pp)
[34] Parker A R 2002 Natural photonic engineers *Mater. Today* **5** 26–31
[35] Yeh P 1988 Optical wave in layered media (New Jersey: Wiley)
[36] Yariv A and Yeh P 2007 *Photonics: optical electronics in modern communications* (New York: Oxford University Press)